Mon. Not. R. Astron. Soc. **000**, 1–7 (2008) Printed 15 September 2008 (MN LATEX style file v2.2)

The population of pulsars with interpulses and the implications for beam evolution

Patrick Weltevrede and Simon Johnston
Australia Telescope National Facility, CSIRO, P.O. Box 76, Epping, NSW 1710, Australia.

arXiv:0804.4318v2 [astro-ph] 15 Sep 2008

Accepted 2008 April 23

ABSTRACT
The observed fraction of pulsars with interpulses, their period distribution and the observed pulse width versus pulse period correlation is shown to be inconsistent with a model in which the angle α between the magnetic axis and the rotation axis is random. This conclusion appears to be unavoidable, even when non-circular beams are considered. Allowing the magnetic axis to align from a random distribution at birth with a timescale of $\sim 7 \times 10^7$ years can, however, explain those observations well. The timescale derived is consistent with that obtained via independent methods. The probability that a pulsar beam intersects the line of sight is a function of the angle α and therefore beam evolution has important consequences for evolutionary models and for estimations of the total number of neutron stars. The validity of the standard formula for the spin-down rate, which is independent of α appears to be questionable.

Key words: pulsars:general — stars:neutron — stars:rotation

1 INTRODUCTION

Pulsars are formed from the supernova explosions which mark the death of high mass stars. During the pulsar birth process, the pulsar's rotation axis is aligned with its velocity vector (Spruit & Phinney 1998; Johnston et al. 2005). A further question arises as to the orientation of the magnetic axis with respect to the rotation axis at birth and the evolution of this angle with time. Over the years, observational evidence seems to support the view that the magnetic and rotation axes align over time (Candy & Blair 1986; Lyne & Manchester 1988; Tauris & Manchester 1998), although there have been claims for no evolution (McKinnon 1993; Gil & Han 1996) and even theoretical reasons for counter-alignment (Beskin et al. 1988). Understanding this issue is important, not only for theoretical considerations of how braking torque works in neutron stars, but also for the evolution of the pulsar beam. This has important implications for evolutionary models and for pulsar surveys generally, such as those planned for the Square Kilometre Array (Kramer et al. 2004).

Radio emission from pulsars arises from a few hundred kilometres above the polar cap, the region bounded by the last open magnetic field lines. It can be shown simply that the radius of the polar cap, r, is related to the pulsar spin period, P, via $r \propto P^{-0.5}$. In turn then, the opening angle of the beam, ρ, can be expressed as

$$\rho = \sqrt{\frac{9\pi \ h_{\rm em}}{2 \ P \ c}} \qquad (1)$$

(e.g Lorimer & Kramer 2005), where $h_{\rm em}$ is the emission height and c the speed of light.

The region bounded by the last open magnetic dipole field lines, and therefore possibly also the pulsar beam, is only circular if the magnetic axis is aligned with the rotation axis and for non-aligned rotators the polar cap is compressed in the plain containing the magnetic and the rotation axis (e.g. Biggs 1990). The beam shape becomes even more complex when the distortion of the magnetic field lines close to the light cylinder is considered (e.g. Romani & Yadigaroglu 1995). Also elongated beam shapes in the latitudinal direction (e.g. Narayan & Vivekanand 1983) as well as an hourglass shape for the beam of the binary pulsar B1913+16 (Weisberg & Taylor 2002) have been proposed.

Observationally, one measures the pulse width ($\Delta\phi$) which is a function of ρ and the geometry of how the line of sight cuts through the beam. Under the assumption that the beam is circular, Gil et al. (1984) derived

$$\sin^2\left(\frac{\Delta\phi}{4}\right) = \frac{\sin^2(\rho/2) - \sin^2(\beta/2)}{\sin(\alpha+\beta)\sin\alpha}, \qquad (2)$$

where α is the angle between the magnetic axis and the rotation axis and β is the impact parameter, the angle between the line of sight and the magnetic axis at its closest approach. Rankin (1990) found that ρ for core emission is correlated with $P^{-1/2}$ by using pulsars with interpulses for which $\alpha \simeq 90^\circ$. Using this correlation in combination with the longitude dependence of the position angle of the linear polarization (Radhakrishnan & Cooke 1969) one can solve α and β for any pulsar with core emission. Several authors

used this method to derive a similar correlation between ρ and P for conal emission (e.g. Rankin 1993; Kramer et al. 1994; Gil et al. 1993). Gould (1994) found the same correlation by using the argument that the most narrow profiles are expected for pulsars with $\alpha \simeq 90^\circ$. The implication of this correlation in conjunction with Eq. 1 is that the emission height and the fraction of the polar cap which is active is independent of the pulsar period (e.g. Mitra & Rankin 2002).

Tauris & Manchester (1998) analysed published values for α of several hundred pulsars, showed they are inconsistent with a random α distribution and concluded that α decreases on a time-scale of $\sim 10^7$ yr. In contrast, McKinnon (1993) concluded that the α distribution is random, provided that the beam was compressed in the latitudinal direction.

In this paper, the issue of beam evolution is approached from a different angle. We do not rely on polarization data or a ρ correlation to determine α and β. Rather, we will construct a beam model based on the observed fraction of pulsars with interpulses and their period distribution and the observed $P - \Delta\phi$ plane is used directly. The interpulse population, the pulse width measurements and the model are described in sections 2, 3 and 4 respectively. The results are presented in section 5 and their implications are discussed section 6.

2 INTERPULSES

The population of pulsars with interpulses is a powerful probe of pulsar beam properties. In the case where an interpulse is seen, with a separation from the main pulse of $\sim 180^\circ$ in rotational phase, it implies that α must be $\sim 90^\circ$ and therefore gives a good count of how many orthogonal rotators there are in the population. We therefore searched the literature to obtain a complete census of the interpulse population. For this search, we excluded all millisecond pulsars and pulsars in globular clusters, because the opening angle of the beams of milli-second pulsars are believed to have a different P dependence to that of normal pulsars (e.g. Kramer et al. 1998) and the values for the spin period derivative ($\dot{P}$) of globular cluster pulsars are contaminated by their acceleration in the gravitational field of the cluster. We started with the catalogue of Taylor et al. (1993) which tabulated 14 interpulse pulsars out of a total of 527 objects. We then examined all pulse profiles in the major surveys conducted since that time.

Table 1 lists the relevant papers, the number of pulsars reported and the interpulses detected. Table 2 lists the population of pulsars with interpulses. The table includes 3 weak interpulses not previously detected. Their profiles will be presented in a forthcoming publication (Weltevrede & Johnston 2008). In total there are 27 pulsars with interpulses from a total sample of 1487 pulsars, i.e. 1.8% of the population. We note that the list should not be considered as complete. Some objects in the list may not be orthogonal rotators but are rather aligned rotators with wide beams (see the debate for PSRs B0950+08 and B1929+10 in Everett & Weisberg 2001 for example). On the other hand we may have missed some interpulse objects because the flux in the interpulse is too weak to be detected.

If the α distribution of pulsars is random, then of the order of 5% of the pulsars can be expected to have an interpulse (e.g. Gil & Han 1996). The measured percentage is lower, indicating a potential problem for such a model. Not only is the percentage of pulsars with interpulses an important clue for beam models, more important still is their period distribution. This distribution is shown in Fig. 1 as a cumulative distribution (thick solid histogram). The dis-

Paper	Ref.	$N_{\rm Pulsars}$	$N_{\rm IP}$
Taylor et al. (1993)	(1)	527	14
Foster et al. (1995)		14	0
Camilo et al. (1996)		19	0
D'Amico et al. (1998)	(2)	84	1
Edwards et al. (2001)		61	0
Manchester et al. (2001)		99	0
Morris et al. (2002)	(3)	119	3
Kramer et al. (2003)	(4)	200	2
Hobbs et al. (2004)	(5)	178	2
Jacoby (2005)		19	0
Lorimer et al. (2005)		8	0
Burgay et al. (2006)		14	0
Lorimer et al. (2006)	(6)	131	2
Manchester et al. (2006)		14	0
Weltevrede & Johnston (2008)	(7)	0	3
Total		1487	27

Table 1. The used literature to find interpulses is listed in the first column. The reference codes are the same as in Table 2. $N_{\rm Pulsars}$ and $N_{\rm IP}$ are the total number of newly discovered normal pulsars in the discussed paper and the number of which have interpulses.

JName	BName	$P\,(s)$	$\dot{P}$	Ref.
J0534+2200	B0531+21	0.0331	4.2×10^{-13}	(1)
J0826+2637	B0823+26	0.5307	1.7×10^{-15}	(1)
J0828–3417	B0826–34	1.8489	1.0×10^{-15}	(1)
J0834–4159		0.1211	4.4×10^{-15}	(4)
J0905–5127		0.3463	2.5×10^{-14}	(7)
J0908–4913	B0906–49	0.1068	1.5×10^{-14}	(1)
J0953+0755	B0950+08	0.2531	2.3×10^{-16}	(1)
J1057–5226	B1055–52	0.1971	5.8×10^{-15}	(1)
J1126–6054	B1124–60	0.2027	2.8×10^{-16}	(7)
J1302–6350	B1259–63	0.0478	2.3×10^{-15}	(1)
J1549–4848		0.2883	1.4×10^{-14}	(2)
J1637–4553	B1634–45	0.1188	3.2×10^{-15}	(7)
J1705–1906	B1702–19	0.2990	4.1×10^{-15}	(1)
J1713–3844		1.6001	1.8×10^{-13}	(4)
J1722–3712	B1719–37	0.2362	1.1×10^{-14}	(1)
J1739–2903	B1736–29	0.3229	7.9×10^{-15}	(1)
J1806–1920		0.8798	1.7×10^{-17}	(3)
J1808–1726		0.2410	1.2×10^{-17}	(6)
J1825–0935	B1822–09	0.7690	5.2×10^{-14}	(1)
J1828–1101		0.0721	1.5×10^{-14}	(3)
J1843–0702		0.1916	2.1×10^{-15}	(5)
J1849+0409		0.7612	2.2×10^{-14}	(6)
J1851+0418	B1848+04	0.2847	1.1×10^{-15}	(1)
J1852–0118		0.4515	1.8×10^{-15}	(5)
J1913+0832		0.1344	4.6×10^{-15}	(3)
J1932+1059	B1929+10	0.2265	1.2×10^{-15}	(1)
J1946+1805	B1944+17	0.4406	2.4×10^{-17}	(1)

Table 2. The 27 interpulses of normal pulsars which can be found in the literature. The reference codes are the same as in Table 1.

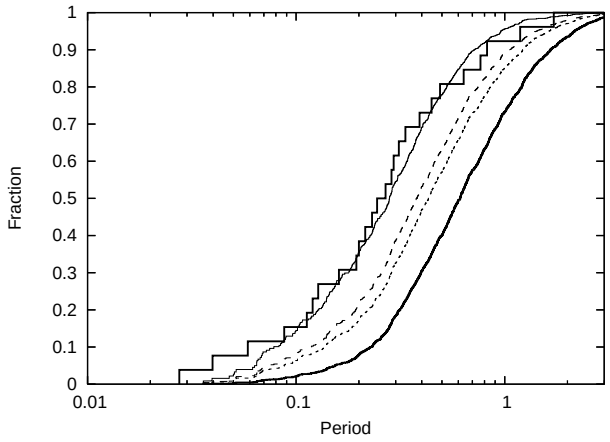

Figure 1. The histogram (thick solid line) shows the observed cumulative distribution of pulse periods of the normal (i.e. non-millisecond) pulsars with interpulses. The lowest (thick) solid curve shows the cumulative period distribution of all normal pulsars. The dotted curve shows the predicted distribution for the pulsars with interpulses in the case of a random α distribution (both for circular and non-circular beams). The dashed and solid curve are for a model including alignment of the magnetic axis for non-circular and circular beams respectively.

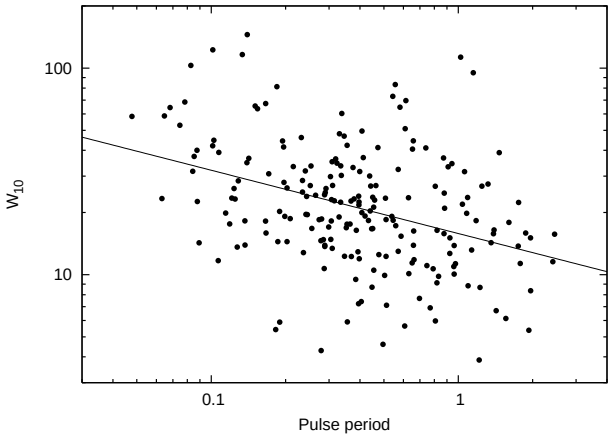

Figure 2. The measured profile 10% widths versus P at an observing frequency around 1390 MHz (Weltevrede & Johnston 2008). Pulsars with a $S/N < 30$ or those with substantial scatter broadening were excluded leaving 205 measurements. The solid line is a power law fit through the data, which has a slope of -0.31, comparable with the fit obtained from the data of Gould & Lyne (1998).

tribution indicates the fraction of pulsars with interpulses y which have a period less than x. Compared with the period distribution of all normal (i.e. non-millisecond) pulsars (lowest thick curve of Fig. 1) there are relatively many more short period pulsars with interpulses. In this paper we will try to construct a geometrical model which can account for the observed statistical properties of the population of pulsars with interpulses.

3 THE OBSERVED PULSE WIDTHS DISTRIBUTION

We have embarked on a long-term timing campaign at the Parkes telescope in Australia to monitor a large sample of young pulsars with high spin-down energy loss rates $\dot{E}$. This sample of pulsars is compared with archival Parkes data, which is published in various papers, in order to determine the differences between pulsars with high and low values for $\dot{E}$ (Weltevrede & Johnston 2008). We refer to that paper for the details of the observations and data reduction.

The dataset is used to determine the correlation between the pulse width $\Delta\phi$ and P. Fig. 2 suggests that the slope in the $\Delta\phi - P$ plane is less steep than $-1/2$. The slope measured by minimizing the χ^2 in log-log space (assuming equal weights) is -0.31 ± 0.05. As pointed out in the introduction, ρ is expected, and found, to be proportional to $P^{-1/2}$. An identical correlation can be expected in the $\Delta\phi - P$ plane, provided that α is independent of P. This measurement is therefore of interest to us because it can be interpreted as evidence for a P dependence of α.

One could argue that the scatter of the points around the correlation in Fig. 2 is so large that a power law with a slope of $-1/2$ would fit the data equally well. We therefore also measured the slope using the measured 10% widths at 1400 MHz by Gould & Lyne (1998), excluding the millisecond pulsars, as a consistency check. Although there is some overlap in our samples, that of Gould & Lyne (1998) contain many northern pulsars which are not present in our sample. The slope measured in the Gould & Lyne (1998) data is also flatter then expected (-0.23 ± 0.06), which makes us more confident that the observed trend is real.

4 THE MODEL

We attempt to explain three observational conclusions by creating a model which is as simple as possible. If one understands the geometry one should first of all be able to construct a model which can predict the observed fraction of pulsars with an interpulse (1.8% or lower, see section 2). Secondly, the model should be able to reproduce the observed period distribution of pulsars with interpulses. Thirdly, the model should explain why the observed $\Delta\phi - P$ correlation is flatter than the expected $P^{-1/2}$ correlation. The effects of a possible alignment timescale of the magnetic axis and non-circular beams will be explored.

The basic approach of this model is to synthesize a population of pulsars in which the $P-\dot{P}$ distribution is identical to the observed distribution. We then assign a random geometry to each pulsar and the subpopulation of pulsars with interpulses is identified using different model assumptions. The statistical properties of the synthesized population of pulsars with interpulses is then compared with the observed population in order to determine which model is able to reproduce the data best.

4.1 The period distribution

The model should first of all reproduce the observed $P - \dot{P}$ distribution for the total observed population of pulsars (those with and without interpulses), which is achieved by simply using the observed $P - \dot{P}$ combinations. Not only does this ensure that the resulting distributions are realistic, it also avoids the necessity to make an full evolutionary

model which would require additional assumptions about pulsar birth properties and their evolution. Note that we are therefore not making any assumptions about the parent distribution that gives rise to the observed distribution of $P-\dot{P}$ combinations. In the next subsection we will describe geometrical factors which could make the period distribution of the pulsars with interpulses different to the total population of observed pulsars.

The catalogue of pulsars maintained by the ATNF[1] (Manchester et al. 2005) was used to obtain the observed $P-\dot{P}$ values. Because the interpulses of milli-second pulsars are not considered in this paper, all pulsars with an estimated surface magnetic field strength below 10^{11} Gauss or a period faster than the Crab were excluded. PSR J1808–1726, with a magnetic field strength of 5.4×10^{10} Gauss, is excluded from the interpulse statistics for consistency. The globular cluster pulsars have unreliable $\dot{P}$ values and are therefore also not considered. Finally, all the pulsars with $P>4$ seconds were removed to exclude the catalogued soft gamma-ray repeaters and the anomalous X-ray pulsars.

4.2 The beam model

The first step is to draw random $P-\dot{P}$ pairs from the total population of observed pulsars as described in Sect 4.1. Secondly, random values are generated for α and β. The magnetic pole and the line of sight are taken to be a random points on a sphere. This implies that the distribution of α and $\zeta=\alpha+\beta$ are sinusoidal. The magnetic axis is allowed to align on a timescale $\tau_{\rm align}$ (Jones 1976)

$$\alpha(t)=\alpha_0\exp\left(-t/\tau_{\rm align}\right), \tag{3}$$

where α_0 is the random α value at birth and t is the age of the pulsar, which is taken to be the characteristic age. The final step is to determine if one or both beams of the pulsar intersect the line of sight given by the randomly generated geometry, which depends on the assumed beam shape. As pointed out in the introduction, different shapes of the polar cap have been proposed. Here we consider only the shape of a polar cap which is bounded by the last open magnetic dipole field lines in order to get a feeling for the effect of non-circular beam shapes. Such a beam is compressed in the plain containing the magnetic and the rotation axis and is roughly elliptic. The axial ratio $\mathcal{E}(\alpha)$ of the ellipse is given by (McKinnon 1993)

$$\mathcal{E}(\alpha)=\cos\delta\sqrt{\cos\left(\alpha-\delta\right)}, \tag{4}$$

where $\delta(\alpha)$ follows from numerically solving

$$2\tan\left(\delta\right)=\tan\left(\alpha-\delta\right). \tag{5}$$

The axial ratio $\mathcal{E}(\alpha)$ varies from 1 (for an aligned beam) to ~0.62 (for an orthogonal beam). Circular beams can be assumed in the model by forcing $\mathcal{E}=1$ for all α.

Apart from the beam shape, a beam size has also to be assumed. For the half opening angle of the beam we use the relation measured by Gould (1994)

$$\rho=5.4^\circ P^{-1/2}, \tag{6}$$

which is consistent with the relation reported by various other authors (e.g. Rankin 1990, 1993; Kramer et al. 1994; Gil et al. 1993). For non-circular beams, ρ of Eq. 6 is taken to be the half opening angle in the longitudinal direction. The conditions for the two pulsar beams to intersect the line of sight are

$$|\beta|\leqslant\mathcal{E}(\alpha)\,\rho \tag{7}$$

and

$$|180^\circ-2\alpha-\beta|\leqslant\mathcal{E}(\alpha)\,\rho. \tag{8}$$

Random values of α and β are generated until at least one of these conditions are met. The width of the pulse profile can then be calculated with Eq. 2 for circular beams.

As noted in section 2, the list of interpulses is not complete for two reasons. The first reason is that some interpulses might have been missed because the flux in the interpulse is too weak to be detected. Extremely weak interpulses could indicate that the pulsar beam just grazes the line of sight. Because the observed ρ (Eq. 6) has been derived considering the 10% pulse widths, beams which just graze the line of sight are not counted as detections in the model (Eqs. 7 and 8). This means that extremely weak interpulses are not accounted for in the model, as well as possibly in the observations. However, some of the observed interpulses will be wide beams of aligned rotators. Therefore the observed interpulse fraction should be considered as an upper limit.

5 RESULTS

Let us start with considering the simplest model, i.e. a random α distribution without alignment ($\tau_{\rm align}=\infty$) and circular beams ($\mathcal{E}(\alpha)=1$). In this scenario our model predicts that 4.4% of the pulsars should have an interpulse, a factor of at least two higher than the observed fraction. This model also clearly fails to explain the observed period distribution of the pulsars with interpulses as the dotted curve of Fig. 1 lies below the observed distribution. This means that there are more short period pulsars with interpulses then predicted. Short period pulsars are expected to have a larger probability to show an interpulse because their beams are wider (Eq. 6), which is the reason why the predicted distribution of pulsars with interpulses (dotted line) lies above the distribution of all pulsars (lowest thick curve). Nevertheless this effect is not enough to explain the observed period distribution of the pulsars with interpulses. The predicted pulse width for this model is correlated with $P^{-0.51}$, very close to the what is expected from Eq. 6. This model therefore fails to explain the three observational properties outlined in section 4.

In order to make the model more accurately reflect the data it is necessary to produce fewer pulsars with interpulses, which can be done by relaxing the condition that forces the beams to be circular. Because the minor axis of non-circular beams is in the plane containing the magnetic and rotation axis, it is less likely that the beams of both magnetic poles intersect the line of sight. This in contrast to elongated beams, which will increase the fraction of pulsars with interpulses and are therefore not considered further here. Indeed, when applying Eq. 4, the predicted fraction of interpulses is decreased to 2.3%. This is still a bit too high,

[1] http://www.atnf.csiro.au/research/pulsar/psrcat

especially as the observed fraction is an upper limit. Because the ellipticity of the beam is independent of P it follows that the predicted pulse period distribution of pulsars with interpulses and the pulse width distribution are identical to the model with circular beams. Therefore the model with non-circular beams also fails to explain the observations.

We next consider the effect of alignment of the pulsar beam. By setting $\tau_{\rm align} = 7 \times 10^7$ years (assuming circular beams) the predicted fraction of pulsars with interpulses drops to the observed value. Also the predicted period distribution of the pulsars with interpulses (thin solid line Fig. 1) now agrees well with the observations, indicating that the model successfully predicts the observed under-abundance of long period pulsars with interpulses. This can be understood because long period pulsars tend to have larger characteristic ages, which means that they tend to be more aligned, which reduces the probability that the beams of both magnetic poles intersect the line of sight. Finally, because the α distribution depends on P in this case, the predicted correlation between $\Delta\phi$ and P will deviate from $-1/2$. The slope of the correlation becomes flatter (the slope is -0.40), as is observed.

Finally, one can consider a model which both includes the ellipticity of the beam and alignment. In that case the timescale of alignment is much longer ($\tau_{\rm align} = 2 \times 10^9$), because both effects reduce the predicted number of interpulses. As a consequence, the predicted period distribution of the pulsars with interpulses (dashed line Fig. 1) does not deviate much from the model without alignment and therefore does not fit the data as well as the model with circular beams.

If pulsar beams align over time, it would imply that the total population of pulsars has an α distribution which is skewed to low values compared with a random distribution. This affects the average beaming fraction because it is a function of α (e.g. Eq. 7 of Tauris & Manchester 1998). The beaming fraction is the fraction of the celestial sphere swept out by the beams of a pulsar, hence it is the probability that a pulsar is observable for a random line of sight. Aligned beams are less likely to intersect the line of sight and are therefore less likely to be observed. The average beaming fraction for the observed population of pulsars, assuming circular beams, is 8.4% and 17% for the model with and without α evolution respectively.

For a random α distribution the fraction of pulsars with beams which continuously intersect the line of sight is tiny (0.01%), because of the α dependence of the beaming fraction in combination with the effect that aligned pulsars are less likely to be formed in the first place. This means that basically no pulsars with extremely wide profiles are expected in the known population of pulsars. This fraction appears too low, as we have already argued that some of the interpulses in Table 2 originate from a single magnetic pole. A more realistic fraction is predicted by the model assuming circular beams including α evolution (1.6%), while $\tau_{\rm align}$ is too long to make a difference in the case of non-circular beams. This can be seen as additional evidence for circular beams and a significant effect of α evolution.

6 DISCUSSION

We have shown that the observed fraction of pulsars with interpulses, their period distribution, the fraction of pulsars with extremely wide profiles and the observed pulse width versus pulse period correlation (as measured in our data and that of Gould & Lyne 1998) is inconsistent with a random α distribution, even when non-circular beams are considered. The main problem is that too many pulsars with interpulses are predicted, especially those with long periods. A number of explanations are possible.

First, one could assume that long period pulsars are less likely to have two active poles. Not only is this assumption ad-hoc, it also does not explain the observed correlation between the pulse width and the pulse period. Our model is kept simple and intuitive by assuming that both magnetic poles always emit radio emission, the beams are directed in exactly opposite directions and have equal widths and luminosities. We therefore aim to find a geometrical solution for the problem.

Secondly, one could assume a different powerlaw relation between ρ and P. In order to correctly predict the number of pulsars with interpulses and their period distribution the observed powerlaw relation (Eq. 6) should be steeper and the constant smaller. This could physically mean that the fraction of the polar cap which is active or the emission height is P dependent. Not only is such a model incompatible with the observations from which Eq. 6 is derived, it also results in a highly unrealistic pulse width distribution (the predicted pulse widths are too narrow and the correlation with P is too steep).

Thirdly, the pulsar beam may not be circular, which is expected if the polar cap is bounded by the last open magnetic field lines. Although elliptical beams which are compressed in the plain containing the magnetic and the rotation axis could help to reduce the number of predicted interpulses, it is not enough. Moreover, the ellipticity is not expected to be P dependent. This implies that this model, like that for circular beams, does not correctly predict the period distribution of the pulsars interpulses and the pulse width period correlation. The fraction of pulsars with extemely wide profiles is also too low.

The only geometrical effect left, as far as we can see, to explain the observations is to relax the assumption that α is random. In order to explain the observed fraction of pulsars with interpulses the α distribution should be skewed to low values. The distribution for short period pulsars should be skewed less than that of long period pulsars in order to explain the observed pulse period distribution of the pulsars with interpulses. The skewness therefore appears to be caused by an *evolution in time* of α rather than by a non-random birth distribution which is fixed in time.

In the previous section it has been shown that the model assuming circular beams can explain the observations well when the magnetic axis is allowed to align from a random distribution at birth with a timescale of $\sim 7\times10^7$ years. The fact that the fraction of pulsars with interpulses, their period dependence, the fraction of pulsars with extremely wide profiles and the pulse width distribution can be explained by adding just one extra model parameter is encouraging. Moreover, by allowing α to evolve it is not necessary to abandon the observed $\rho - P$ relation (Eq. 6) or to resort in ad-hoc

assumptions about magnetic poles which are not always active.

The timescale is comparible with the timescale derived from the observed α distribution by Tauris & Manchester (1998). Measuring α is far from trivial and for most pulsars it is, at best, only poorly constrained. It should be stressed that although we discuss α evolution, we do not rely on (indirect) measurements of α. Therefore our results are an important addition to the existing evidence for alignment.

The pulse period distribution of the pulsars with interpulses can be used to distinguish between beam shapes. The data show that the derived distribution assuming circular beams fits the data better than that assuming elliptical beams. This suggests that the beams are more circular than expected from a simple model which has the polar cap bounded by the last open dipole magnetic field lines. For example, more complicated models which take into account the distortion of the magnetic field lines close to the light cylinder predict roughly circular beams (e.g. Romani & Yadigaroglu 1995).

Our estimation of $\tau_{\rm align}$ should be considered to be very rough because of a number of reasons. First of all, the timescale is based on the observed characteristic age distribution of pulsars. The characteristic age should be considered to be only a rough estimator of the true age, because the details of pulsar spin-down are not well understood. Secondly, the α evolution could have a different form than the assumed exponential decay. For instance one could imagine that the decay rate is a function of α. Thirdly, $\tau_{\rm align}$ also depends on the shape of the radio beam. If the beam is non-circular then $\tau_{\rm align}$ should be larger in order to explain the observations. Finally, the timescale is based on the observed fraction of interpulses. It is assumed that all the observed interpulses are caused by emission from the opposite pole, which is unlikely to be the case. Therefore the observed fraction of pulsars with interpulses should be seen as an upper limit, resulting in an overestimation of $\tau_{\rm align}$.

Although our estimated value of $\tau_{\rm align}$ is very rough, the observations can only be explained if the effect of alignment is important and therefore happens on a timescale comparable to the age of a typical pulsar. Beam evolution has some important consequences for population studies, evolutionary models and pulsar searches, for two reasons.

The first is that the beaming fraction depends on $\tau_{\rm align}$ such that aligned beams are less likely to intersect the line of sight. Therefore a consequence of alignment of pulsar beams over time is that older pulsars become harder to find, hence the inferred total population of old pulsars should be larger. The average beaming fraction for the observed population of pulsars, assuming circular beams, is 8.4% and 17% for the model with and without α evolution respectively. Therefore the inferred total population of pulsars is about twice as high when α evolution is considered.

Secondly, one can ask the more fundamental question of what alignment implies for the spin-down of pulsars. The evolution of α must be the result of the braking torque, hence it is related to the spin-down of pulsars. If the torque changes α, it seems reasonable that the torque also depends on α. It is therefore not unlikely that the pulsar spin-down itself has an α dependence. The spin-down of a rotating dipole field in a vacuum depends on α ($\dot{E} \propto \sin^2\alpha$, e.g. Jackson 1962), but how different this is in the presence of a pulsar magnetosphere is unclear. An α dependent spin-down implies that the magnetic field strength, the characteristic age and spin-down energy loss rate of a pulsar also depends on α, which has important consequences for evolutionary models and population studies.

We have shown that the observed population of pulsars with interpulses places strong restrictions on beam models. Future instrumentation, such as the Square Kilometre Array, will greatly enlarge the observed population of pulsars, enabling the possibility to distinguish between models with different beam shapes and different functional forms for the α evolution. This will contribute to a better understanding of how breaking torques in neutron stars work.

ACKNOWLEDGMENTS

The Australia Telescope is funded by the Commonwealth of Australia for operation as a National Facility managed by the CSIRO. We would like to thank the referee for his/her constructive comments.

REFERENCES

Beskin V. S., Gurevich A. V., Istomin Y. N., 1988, Ap&SS, 146, 205
Biggs J. D., 1990, MNRAS, 245, 514
Burgay M., Joshi B. C., D'Amico N., Possenti A., Lyne A. G., Manchester R. N., McLaughlin M. A., Kramer M., Camilo F., Freire P. C. C., 2006, MNRAS, 368, 283
Camilo F., Nice D. J., Shrauner J. A., Taylor J. H., 1996, ApJ, 469, 819
Candy B. N., Blair D. G., 1986, ApJ, 307, 535
D'Amico N., Stappers B. W., Bailes M., Martin C. E., Bell J. F., Lyne A. G., Manchester R. N., 1998, MNRAS, 297, 28
Edwards R. T., Bailes M., van Straten W., Britton M. C., 2001, MNRAS, 326, 358
Everett J. E., Weisberg J. M., 2001, ApJ, 553, 341
Foster R. S., Cadwell B. J., Wolszczan A., Anderson S. B., 1995, ApJ, 454, 826
Gil J. A., Gronkowski P., Rudnicki W., 1984, A&A, 132, 312
Gil J. A., Han J. L., 1996, ApJ, 458, 265
Gil J. A., Kijak J., Seiradakis J. H., 1993, A&A, 272, 268
Gould D. M., 1994, PhD thesis, University of Manchester
Gould D. M., Lyne A. G., 1998, MNRAS, 301, 235
Hobbs G., Faulkner A., Stairs I. H., Camilo F., Manchester R. N., Lyne A. G., Kramer M., D'Amico N., Kaspi V. M., Possenti A., McLaughlin M. A., Lorimer D. R., Burgay M., Joshi B. C., Crawford F., 2004, MNRAS, 352, 1439
Jackson J. D., 1962, Classical Electrodynamics. Wiley
Jacoby B. A., 2005, PhD thesis, California Institute of Technology, United States – California
Johnston S., Hobbs G., Vigeland S., Kramer M., Weisberg J. M., Lyne A. G., 2005, MNRAS, 364, 1397
Jones P. B., 1976, Astrophys. Space Sci., 45, 369
Kramer M., Backer D. C., Lazio T. J. W., Stappers B. W., Johnston S., 2004, New Astron. Rev., 48, 993
Kramer M., Bell J. F., Manchester R. N., Lyne A. G., Camilo F., Stairs I. H., D'Amico N., Kaspi V. M., Hobbs

G., Morris D. J., Crawford F., Possenti A., Joshi B. C., McLaughlin M. A., Lorimer D. R., Faulkner A. J., 2003, MNRAS, 342, 1299
Kramer M., Wielebinski R., Jessner A., Gil J. A., Seiradakis J. H., 1994, A&AS, 107, 515
Kramer M., Xilouris K. M., Lorimer D. R., Doroshenko O., Jessner A., Wielebinski R., Wolszczan A., Camilo F., 1998, ApJ, 501, 270
Lorimer D. R., Faulkner A. J., Lyne A. G., Manchester R. N., Kramer M., McLaughlin M. A., Hobbs G., Possenti A., Stairs I. H., Camilo F., Burgay M., D'Amico N., Corongiu A., Crawford F., 2006, MNRAS, 372, 777
Lorimer D. R., Kramer M., 2005, Handbook of Pulsar Astronomy. Cambridge University Press
Lorimer D. R., Xilouris K. M., Fruchter A. S., Stairs I. H., Camilo F., Vazquez A. M., Eder J. A., McLaughlin M. A., Roberts M. S. E., Hessels J. W. T., Ransom S. M., 2005, MNRAS, 359, 1524
Lyne A. G., Manchester R. N., 1988, MNRAS, 234, 477
Manchester R. N., Fan G., Lyne A. G., Kaspi V. M., Crawford F., 2006, ApJ, 649, 235
Manchester R. N., Hobbs G. B., Teoh A., Hobbs M., 2005, AJ, 129, 1993
Manchester R. N., Lyne A. G., Camilo F., Bell J. F., Kaspi V. M., D'Amico N., McKay N. P. F., Crawford F., Stairs I. H., Possenti A., Morris D. J., Sheppard D. C., 2001, MNRAS, 328, 17
McKinnon M. M., 1993, ApJ, 413, 317
Mitra D., Rankin J. M., 2002, ApJ, 577, 322
Morris D. J., Hobbs G., Lyne A. G., Stairs I. H., Camilo F., Manchester R. N., Possenti A., Bell J. F., Kaspi V. M., Amico N. D., McKay N. P. F., Crawford F., Kramer M., 2002, MNRAS, 335, 275
Narayan R., Vivekanand M., 1983, A&A, 122, 45
Radhakrishnan V., Cooke D. J., 1969, Astrophys. Lett., 3, 225
Rankin J. M., 1990, ApJ, 352, 247
Rankin J. M., 1993, ApJ, 405, 285
Romani R. W., Yadigaroglu I.-A., 1995, ApJ, 438, 314
Spruit H., Phinney E. S., 1998, Nature, 393, 139
Tauris T. M., Manchester R. N., 1998, MNRAS, 298, 625
Taylor J. H., Manchester R. N., Lyne A. G., 1993, ApJS, 88, 529
Weisberg J. M., Taylor J. H., 2002, ApJ, 576, 942
Weltevrede P., Johnston S., 2008, MNRAS, in prep.